Jurnal Teknologi

Full Paper

ANALYSIS OF TEMPERATURE SENSOR IN ALL-PASS MICRORING RESONATOR

Azam Mohamad[a*], Mahdi Bahadoran[a,b], Suzairi Daud[a,b], Kashif Tufail Chaudhary[a,b], M. S. Aziz[a,b], M. A. Jalil[b], Jalil Ali[b], P. P. Yupapin[c]

[a]Laser Center, Ibnu Sina Institute for Scientific & Industrial Research, Universiti Teknologi Malaysia, 81310 UTM Johor Bahru, Johor, Malaysia
[b]Department of Physics, Faculty of Science, Universiti Teknologi Malaysia, 81310 UTM Johor Bahru, Johor, Malaysia
[c]Nanoscale Science and Research Alliance, Faculty of Science, King Mongkut's Institute of Technology, Ladkrabang, Bangkok 10520, Thailand

Article history
Received
15 August 2015
Received in revised form
15 November 2015
Accepted
30 December 2015

*Corresponding author
azam.mohd88@gmail.com

Graphical abstract

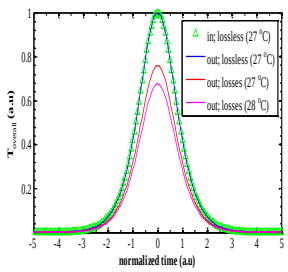

Abstract

The temperature sensor using all-pass microrin resonator (APMRR) investigated theoretically and analyzed. An optical bright soliton is used as a probe to study the effect of applied temperature on the light behavior pass through microring waveguide. The split-step Fourier method is used to study the pulse propagation inside the APMRR. Result shows that the rise of temperature on peak amplitude ratio fit with quadratic line in temperature range of 27 °C-37 °C. . The temperature at 30 °C generate higher slope of reduction compare to temperature at 36oC. The amplitude ratio is reduced into 0.6 (-4.4370 dB) when the temperature increased as small as 1 °C. The operating range for all-pass resonator is 97 °C with amplitude reduction of -8.3975 dB.

Keywords: SOI waveguide, ring resonator, temperature sensing, Split-Step Fourier method

Abstrak

Sensor suhu menggunakan semua-pass resonator microring (PALMER) menyiasat secara teori dan dianalisis. Soliton optik terang digunakan sebagai siasatan untuk mengkaji kesan suhu digunakan ke atas tingkah laku cahaya melalui microring pandu gelombang. Kaedah Fourier berpecah-langkah yang digunakan untuk mengkaji pembiakan nadi di dalam PMR. Keputusan menunjukkan bahawa kenaikan suhu di puncak nisbah amplitud patut dengan garis kuadratik dalam julat suhu daripada suhu 27-37 °C. . Suhu pada 30 °C menjana cerun yang lebih tinggi berbanding dengan pengurangan suhu pada 36oC. Nisbah amplitud dikurangkan ke 0.6 (-4,4370 dB) apabila suhu meningkat sekecil 1 °C. Julat operasi untuk semua-pass resonator adalah 97 °C dengan pengurangan amplitud -8,3975 dB.

Kata kunci: Pandu gelombang SOI, cincin resonator, suhu sensing, kaedah Fourier Split-Langkah

1.0 INTRODUCTION

The Fabry-Perot and Mach-Zenhder interferometer are the popular transducer for temperature sensing [1-4]. Both interferometer measure temperature fluctuation versus wavelength variations. Same as interferometers, another device consist a bus and ring waveguide that both waveguides are vertically coupled (Figure 1) can be used for temperature sensing. This configuration is known as all-pass microrin resonator (APMRR) mostly work based on a change in wavelength and cavity length to describe the temperature effect [5-8]. Considering the change on the extinction ratio is another way in temperature measurement [9]. In contrary with the conventional temperature sensors that use a multi-wavelength source for temperature sensing, here we use soliton pulse as a probe to measure temperature variations. Waveguide material plays a crucial role in obtaining the soliton pulse since the dispersion and nonlinearity required to be balanced in the medium to satisfy the prerequisite condition for optical soliton formation [10-17]. The optical soliton has been used in force sensors[18, 19], bio sensing[17], drug delivery[13, 14], optical switching[20-22] and multi-soliton generation [18, 23-26].

In this paper, a temperature sensor is demonstrated using a vertical coupling all-pass microring resonator. A reason using a vertical coupling is to focus only on the ring section. A bright pulse with coherent wavelength is used as an input source of the device with low repetition rate. The device is designed by developing a mathematical model of the sensor and use a silicon waveguide material to fulfil the requirement for maintain soliton pulse formation. The analysis on temperature sensor in all-pass resonator is the aim of the research.

2.0 THEORETICAL AND BACKGROUND

Microring resonators have shown great potential in optical communication and photonics sensors [17-22, 27-31]due to their compactness, good performance high sensitivity and low cost of fabrication. Analysis of temperature effect in all-pass resonator is started by developing a pulse propagation model within microring resonator including the effect of absorptions. All-pass microring resonator sensor (APMRR) is illustrated in Figure 1. A bright soliton as a probe is fed into the input port of resonator and the condition fulfilled for soliton formation within the medium if the effect of anomalous dispersion and nonlinearity remain in balance [32]. A mathematical model of bright soliton pulse is symbolized as

$$E_{in} = \sec h\left(\frac{t}{T_o}\right) \tag{1}$$

Here T_o shows the initial pulse width. Since the silicon contains a various types of absorptions that degrade device performance for optical soliton formation. The pulse propagation within silicon can be described in the form of nonlinear Schrödinger equation (NLSE) that determine the silicon as a nonlinear material [1, 2]. The NLSE is given by[3]

$$\frac{\partial E}{\partial z} + \frac{i\beta_2}{2}\frac{\partial^2 E}{\partial t^2} = i\gamma P_o E - \alpha_{tot} E \,. \tag{2}$$

Here E is electric field and P_0 shows the output pulse power. The anomalous dispersion and nonlinearity are described by the group velocity dispersion β2 and γ as nonlinear Kerr coefficient. A total absorptions of silicon is represented as α_{tot} which composed by the linear loss(lin), thermal absorption (TA), two-photon absorption (TPA)[4] and free-carrier absorption (FCA)

$$\alpha_{tot} = \alpha_{lin} + \alpha_{TA} + \alpha_{TPA} + \alpha_{FCA} \tag{3}$$

The two-photon absorption α_{TPA} is the process of photon absorption that excites an electron from valence band into conduction band resulting accumulative electron concentration inside modal area. The process of two-photon absorption is given by

$$\alpha_{TPA} = \frac{\gamma n_{core} \beta_{TPA} P_o}{k_o n_2} \,. \tag{4}$$

Here the n_{core}, n_2, γ, β_{TPA}, P_o, and k_o are the core refractive index, nonlinear refractive index, nonlinear Kerr coefficient, TPA coefficient, pulse peak power, and vacuum propagation constant, respectively. An accumulative electron concentration creates an additional loss that absorbs another photon for another excitation process of electron called the free-carrier absorption (FCA) [5]

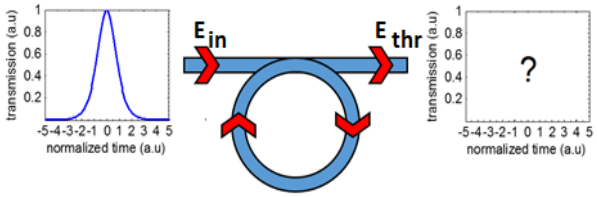

Figure 1 Schematic illustration of the pulse propagation along all-pass microring resonator. The E_{in}, E_{thr} are input and through put electric fields

The carrier generation inside modal area is given by

$$N_{electron} = \frac{\beta_{TPA} P_o^2(z)\tau_{eff}}{2h\nu_o A_{eff}^2} \,. \tag{5}$$

Here, $N_{electron}$ is the carrier concentration of electron that is used for estimating the production of carrier concentration inside modal area. A_{eff}, β_{TPA}, and P_o represent effective mode core area of waveguide, two-photon absorption coefficient, and pulse peak power, respectively. τ_{eff} shows the effective carrier

recombination lifetime which is a limiting factor for nonlinearity and the term hv_o represents a single photon energy used by electron for excitation.

The rise of the carrier concentration produces another absorption process known as free-carrier absorption FCA which is given by

$$\alpha_{FCA} = \sigma_{FCA} N_{electron} . \quad (6)$$

where σ_{FCA} is a cross-section of free-carrier absorption. Carrier generation inside modal area can be minimized if the pulse operate at low repetition rates. Lower repetition rates make pulse travels in resonator just like a single pulse [6]. For this case the recombination lifetime is governed by the pulse width since the pulse width is shorter than the effective carrier recombination lifetime τ_{eff}. High intensity produce high nonlinearity and the phenomenon occur when the two pulses collide at the same time and direction resulting a constructive interference. Surface roughness of the silicon will make another additional loss in which the losses by surface roughness is represented as linear loss α_{lin}. Soliton formation in all-pass resonator also distorted by temperature. Temperature effect on device occurs based on change of refractive index under the temperature variations produce an index deformation Δn_Θ that is shown as [7]

$$\Delta n_\theta = \kappa_\theta \cdot \Delta T . \quad (7)$$

The change on refractive index is depend on the thermo-optic coefficient $k\Theta$ and temperature changing factor ΔT. The temperature changing factor can be related to time and determined by the variation of cavity width as [8]

$$\Delta T = T_{\max}\left(1-\exp\left[\frac{-t}{\tau_T}\right]\right). \quad (8)$$

where T_{max} is the maximum temperature increase , t shows time and τ_T is the thermal time constant which is given by

$$\tau_T = \frac{\rho_{Si} C_{Si} w_c^{\,2}}{\kappa_{Si}\pi^2} \quad (9)$$

where the ρ_{Si}, C_{Si}, κ_{Si}, and w_c are the silicon cavity mass density, specific heat, thermal conductivity, and cavity width of ring, respectively. The index deformation may also create an additional loss which known as a thermal absorption (TA) loss which is given

$$\alpha_{TA} = \frac{4\pi \cdot n_I}{\lambda_{core}} \quad (10)$$

where the thermal absorption TA is symbolized as α_{TA}, imaginary part of refractive index is n_I and ,the input wavelength λ_{core} is another parameter that relate with TA.

3.0 RESULTS AND DISCUSSION

A 10 picosecond probe soliton pulse with the repetition rate of 0.232 ps is launched into the input port of all-pass microring resonator (APMRR) fabricated from the anomalous-dispersive and nonlinear silicon material. Table 1 shows the values of device and pulse parameters employed in our study. The pulse propagation along APMRR described using Split-step Fourier Method and analysis is made by Matlab software. A schematic diagram for one roundtrip soliton pulse propagation within the APMRR with considering the total losses are demonstrated in Figure 2 and the simulated result are shown in Figure 3.

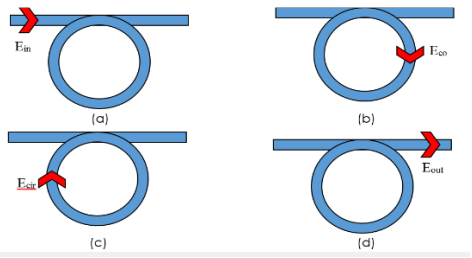

Figure 2 Schematic illustration on pulse propagation along all-pass resonator. The terms E_{in}, E_{co}, E_{cir}, and E_{out} are represented the amplitude of input, half ring, ring, and output fileds

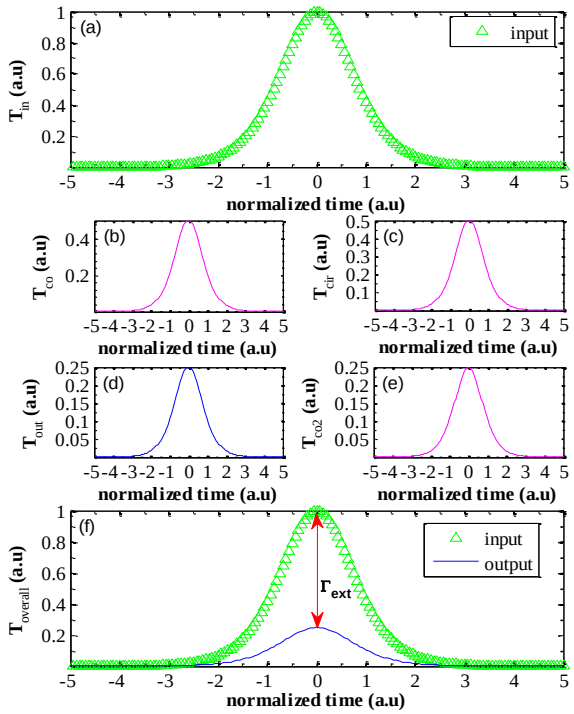

Figure 3 Soliton pulse propagation within all-pass microring resonator. A purple line represents the pulse propagation along the APMRR

As shown in Figure 2(a), the soliton pulse starts propagating in bus waveguide. The correspondent result for this state is simulated pulse shape is represented as a secant-hyperbolic with normalized peak amplitude of 1 in Figure 3(a). When the soliton pulse meet the coupling region, as shown in Figure 2(b), its amplitude decreases. The reduction of amplitude is related to the coupling coefficient .Since 3dB coupling (k = 0.5) is selected for our sensor the amplitude decreases into half of its peak amplitude as shown in Figure 3(b). The amplitude remain unchanged while travels along APMRR (Figure 3(c)).

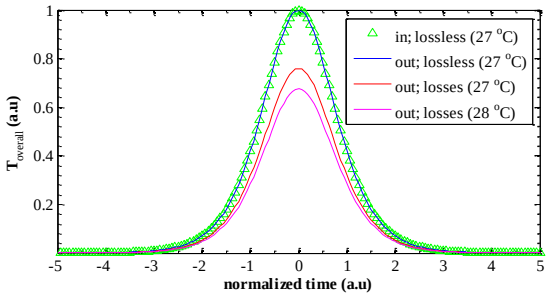

Figure 4 Soliton pulse propagation in 25 roundtrip within all-pass microring resonator in resonance condition. The effect of considering absorptions shows in red and the effect of temperature variation is shown in magenta line

Table 1 Simulation parameters of all-pass resonator sensor for 3dB coupling

Parameter name	Symbol	Value	Reference
Nonlinear index	n_2	6×10^{-18} m^2/W [40]	[40]
TPA coefficient	β_{TPA}	5×10^{-12} m/W [34]	[34]
Wavelength	λ_{core}	1.55μm	
Effective mode area	A_{eff}	0.13 μm^2 [41]	[41]
Nonlinear coefficient	γ	187.0924 W^{-1}/m	
FCA cross section	σ_{FCA}	1.45×10^{-21}m^2 [34]	[34]
Linear propagation loss	α_{lin}	22 dB/m	
Pulse width	T_o	10 ps	
Cavity Width	w_c	660 nm	
Cavity Ring	R	20 μm	
Group velocity dispersion	β_2	-26.83 ps^{2}mm^{-1}	
Input peak power	P_o	1 Watt	
Core index	n_{core}	3.48 [42]	[42]
Silicon cavity mass density	ρ_{Si}	2.33 g/cm^3 [39]	[39]
Specific heat	C_{Si}	0.7 J/g.K [39]	[39]
Thermal conductivity	κ_{Si}	1.3 J/cm.s.K [39]	[39]
Thermal dissipation time	τ_θ	1 μs [38]	[38]
Thermo-optic coefficient	κ_θ	1.86x10^{-4}K^{-1}	[38]

The value of amplitude remain unchanged because the effect of dispersion and nonlinearity are balanced in which the anomalous dispersion compensate the nonlinearity of the silicon. In Figure 2(d), the amplitude begin to decrease again into 0.25. Result shows another power reduction during in feedback (Figure 3(d)). The important note from overall results is the soliton pulse reduce its power when travels along APMRR but the secant-hyperbolic profile still maintain during propagation. The extinction ratio $\Gamma_{EXT} = T_{out}/T_{in}$ is the parameter to measure the power reduction of APMRR where T_{out} and T_{in} are the terms of transmission at output and input ports, respectively. The extinction ratio from this resonator is 0.25 and in decibel unit of the extinction ratio is -12.0412 dB. The power reduction still occurs in the resonator in spite of lossless condition because of the coupling effect at coupling region. The coupling effect is shown in Figure 3(b) which the pulse power reduces to the half value as it was inputted. Other half of the power continue travelling along bus waveguide and this power is considered as a waste.

Table 2 Slope of reduction for all-pass microring resonator in the range of 27°C-37°C

Through port	Tangent line	Single source: Slope of reduction (dB°C^{-1})	Temperature (°C)
	1st	-0.6150	30
	2nd	-0.1244	36

When implement a condition of pulses with multiple roundtrip, a compensation of amplitude occurs as shown in Figure 4. When pulses propagate in 25 roundtrip, soliton pulse will reach the same level as inputted. The pulse reduces its amplitude to 0.7 (-3.0980 dB) when losses of silicon is considered. The losses of the resonator stems in the linear loss (lin), two-photon absorption (TPA), and free-carrier absorption (FCA). The increase in temperature creates an additional loss to the APMRR. Increase of temperature as small as 1 oC causes the extra amplitude reduction of 0.6 (-4.4370 dB).

Figure 5 shows the light transmission via APMRR against temperature. It shows the effect of amplitude pulse on the variation of temperature. In this case the 3 dB coupling and pulses propagation in resonance condition are applied. Result shows decreases of transmission against temperature. The lower amplitude pulse measured when temperature rise up from 27 °C to 87 °C as depicts in Figure 5(a).

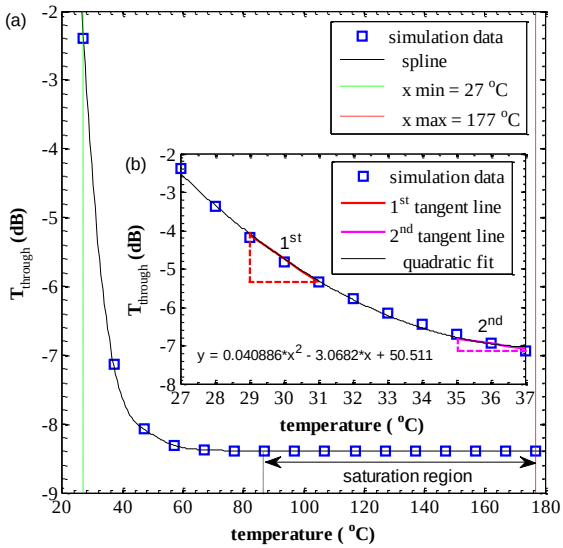

Figure 5 Transmission versus temperature for all-pass microring resonator

A spline line is fitted to the result and unexpected finding achieved where amplitude reduction reach its threshold detection at 97°C with amplitude reduction of -8.3975 dB. After reaching its threshold, amplitude pulse remains unchanged for the temperature range above 97 °C. Scaling down the temperature between 27-37 °C shown in Figure 5(b). The system behavior in this operating range of temperature is corresponded to a quadratic line. Because of quadratic response this area we divided this range into the partitions with the temperature variation as small as 1°C in which each partition has its own slope of reduction. Slope of reduction is estimated by determining tangent line. In Figure 5(b), two tangent lines are required for measuring slope differences. The point of 30 °C is used as the first tangent line 5and 36 °C is considered for the second tangent line. Slope of reduction for 30 °C and 36 °C are displayed by Table 2. Result shows the higher slope of reduction is produced by 30 °C than 36 °C. In Figure 5(b) there is a clear trend of decreasing on slope of reduction when raise temperature.

4.0 CONCLUSION

In summary, the all-pass microring resonator is proper candidate for temperature sensing in term of amplitude change. The soliton pulse undergoes the power reduction when travels across all-pass microring resonator. The power reduction is due to the total lossesand absorptions of silicon waveguide material. The temperature fluctuation create an additional loss to the system. In this system, the pulse power is reduced to 0.6 (-4.4370 dB) when temperature increased by 1°C. An amplitude reduction is determined by slope of reduction. Result shows that temperature at 30 °C generate higher slope of reduction compare to temperature at 36 °C which can be used in thermal sensors.

Acknowledgement

This research is fully supported by UTM_PAS grant (Q.J130000.2709.01K77). The authors fully acknowledged Universiti Teknologi Malaysia for the approved fund.

References

[1] Lu, P., Men, L., Sooley, K. and Chen, Q. 2009. Tapered Fiber Mach–Zehnder Interferometer for Simultaneous Measurement of Refractive Index and Temperature. *Applied Physics Letters*. 94: 31110.
[2] Chen, X., Shen, F., Wang, F., Huang, Z. and Wang, A. 2006. Micro-Air-Gap Based Intrinsic Fabry-Perot Interferometric Fiber-Optic Sensor. *Applied Optics*. 45: 7760-7766.
[3] Zhu, Y. Z., Huang, Z. Y., Shen, F. B. and Wang, A. B. 2005. Sapphire-Fiber-Based White-Light Interferometric Sensor for High-Temperature Measurements. *Optics Letters*. 30: 711-713.
[4] Kim, D. W., Shen, F., Chen, X. and Wang, A. 2005. Simultaneous Measurement of Refractive Index and Temperature Based on a Reflection-Mode Long-Period Grating and an Intrinsic Fabry-Perot Interferometer Sensor. *Optics Letters*. 30: 3000-3002.
[5] Padgaonkar, V., Arbor, A., Lipson, M. and Pradhan, S. 2004. Thermal Effects in Silicon Based Resonant Cavity Devices. *NNIN REU Research Accomplishments*. 98-99.
[6] Kwon, M. S. and Steier, W. H. 2008. Microring-Resonator-Based Sensor Measuring Both the Concentration and Temperature of a Solution. *Optics Express*. 16: 9372-9377.
[7] Kiyat, I., Aydinli, A. and Dagli, N. 2006. Low-Power Thermooptical Tuning of SOI Resonator Switch. *IEEE Photonics Technology Letters*. 18: 364-366.
[8] Kim, G. D., Lee, H. S., Park, C. H., Lee, S. S., Lim, B. T., Bae, H. K. and Lee, W. G. 2010. Silicon Photonic Temperature Sensor Employing a Ring Resonator Manufactured Using a Standard CMOS Process. *Optics Express*. 18: 22215-22221.